2014

Suppression of Raman Soliton Self-frequency Shift in Photonic Cystal Fibers with Tellurite Subwavelength Core

Shua Wei
Beijing University of Posts and Telecommunications

Jinhui Yuan
Beijing University of Posts and Telecommunications

Chongxiu Yu
Beijing University of Posts and Telecommunications

See next page for additional authors

Recommended Citation

Wei, S., Yuan, J., Yu, C., Li, S., Jin, B., Hu, X., Farrell, G. and Qiang Wu:Suppression of Raman Soliton Self-frequency Shift in Photonic Cystal Fibers with Tellurite Subwavelength Core. *Optical Engineering*, 53 (5), 2014. doi:10.1117/1.OE.53.5.056109

Optical Engineering

SPIEDigitalLibrary.org/oe

Suppression of Raman soliton self-frequency shift in photonic crystal fibers with tellurite subwavelength core

Shuai Wei
Jinhui Yuan
Chongxiu Yu
Sha Li
Boyuan Jin
Xiaoming Hu
Gerald Farrell
Qiang Wu

Suppression of Raman soliton self-frequency shift in photonic crystal fibers with tellurite subwavelength core

Shuai Wei,[a] Jinhui Yuan,[a,*] Chongxiu Yu,[a] Sha Li,[a] Boyuan Jin,[a] Xiaoming Hu,[a] Gerald Farrell,[b] and Qiang Wu[b]
[a]Beijing University of Posts and Telecommunications, State Key Laboratory of Information Photonics and Optical Communications, P.O. Box 163, 100876 Beijing, China
[b]Dublin Institute of Technology, School of Electronic and Communications Engineering, Photonics Research Center, Kevin Street, Dublin 8, Ireland

Abstract. A new nonlinear evolution equation including the vector nature of the electromagnetic field and the frequency variation of the mode profile is derived. A kind of new nonlinearity is demonstrated. Its magnitude is strongly dependent on the waveguide geometrical parameters, which will lead to a suppression of the Raman soliton self-frequency shift in a photonic crystal fiber with a tellurite subwavelength core. Our results can be supported by the detailed numerical simulations. [DOI: 10.1117/1.OE.53.5.056109]

Keywords: Raman soliton self-frequency shift; tellurite glass; photonic crystal fibers; geometrical nonlinearity.

Paper 140146 received Jan. 31, 2014; revised manuscript received Apr. 7, 2014; accepted for publication Apr. 24, 2014; published online May 19, 2014.

1 Introduction

Photonic crystal fibers (PCFs) have attracted great attention due to their unique optical characteristics, such as tailored dispersion and high nonlinearity, and so on.[1–6] Several nonlinear effects, including self-phase modulation (SPM), Raman-stimulated Raman scattering, Raman soliton self-frequency shift (RSSFS), soliton fission, and the dispersive wave in PCFs have been deeply studied for applications in laser sources of different wavebands.[7–12]

Recently, because of the progress on new fabrication techniques, lots of interests have been concentrated on the non-silica glasses with wider infrared transmission windows, such as tellurite, fluoride, and chalcogenide glasses. Tellurite glasses possess a higher nonlinear refractive index than that of silica glass by at least one order of magnitude. Because of the huge relative index difference caused by the tellurite glass core, the PCFs with the tellurite subwavelength core can form a very small effective mode area and show a higher Kerr nonlinear coefficient. Moreover, the tellurite glasses have good chemical and thermal stability. Therefore, they become the suitable material for nonlinear studies in the near-infrared region.[13–15]

The conventional generalized nonlinear Schrodinger equation (GNLSE) can exactly analyze the pulse propagation in PCFs with a larger core size on the assumption that the longitudinal component of the electric field is beyond consideration compared with the transverse components. When the core diameter is sufficiently small or the refractive index contrast between core and cladding is gradually increased, the longitudinal component of the electric field of the fundamental mode becomes more obvious and must be considered in GNLSE. In a recent study, taking into account the vector natures of electromagnetic field and the frequency dependence of the fundamental mode in the photonic nanowires with a subwavelength core diameter, a new equation is used to describe the pulse propagation.[16] The simulation results by the new propagation equation show the suppression of a new nonlinearity on RSSFS by comparing it with that obtained by the conventional GNLSE. However, the PCF is based on silica in Ref. 16, which has a much lower nonlinearity than that of tellurite glass. In order to ensure the new pulse propagation equation and the numerical simulations are more precise, a PCF with a nanoscale core formed by the high index glass to enhance the new nonlinearity is necessary. In addition, Ref. 16 just primarily studies the self-frequency shift of high-order solitons, where the influences of the pulse temporal width and transmission distance are not considered. Moreover, the very important parameters of fiber absorption, the third-order dispersion for the Raman soliton propagation, and the suppression degree of RSSFS are not considered.

In this article, the pulse propagation inside the PCF with a nanoscale tellurite glass core is studied. The z-component of the electric field and the sensitivity of mode distribution on the frequency are considered due to the tight field confinement. The fiber absorption and the third-order dispersion coefficient are taken into account to accurately show the evolution of the short pulse inside the PCF. A kind of new nonlinear geometrical nonlinearity emerges. By adjusting the PCF structure and decreasing the core size, the geometrical nonlinearity can compete with the Raman effect in a specific wavelength range. The suppression of the geometrical nonlinearity on the fundamental soliton is demonstrated based on the new propagation equation. At different pulse powers, pulse temporal width, and transmission distance, the suppression of RSSFS is demonstrated.

2 Photonic Crystal Fiber Characteristics

The PCF structure designed is shown in Fig. 1(a), where the red circle is the central core of the tellurite glass T2 [77TeO2-10Na2O-10ZnO-3PbO (%mol)],[17] which has a refractive index $n = 2.078$ and a nonlinear index $n_2 \approx 5.9\times 10^{-19}$ m^{-1} W^{-1}. n_2 is almost 23 times larger than that of silica. The blue cladding region with hexagon air holes is

*Address all correspondence to: Jinhui Yuan, E-mail: yuanjinhui81@163.com

0091-3286/2014/$25.00

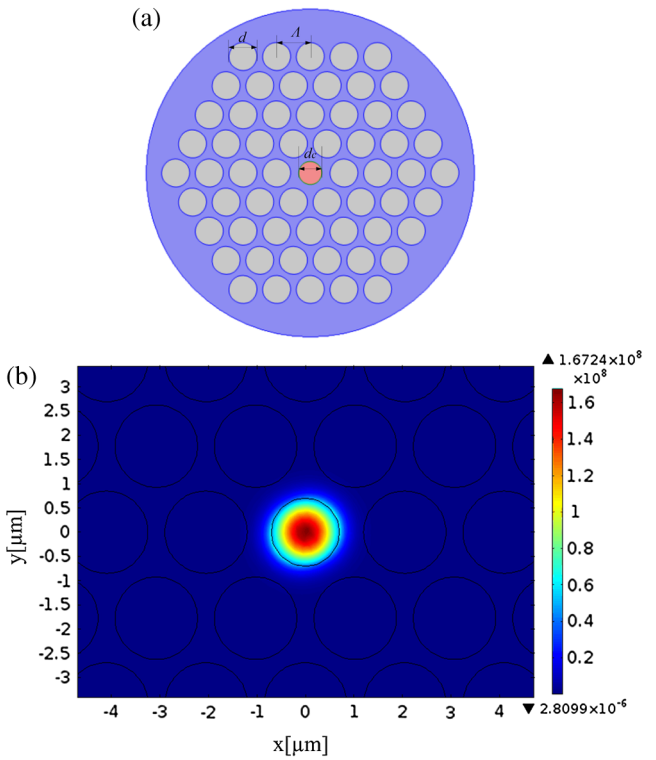

Fig. 1 (a) The structure of the proposed photonic crystal fiber (PCF), and (b) the fundamental mode intensity at the wavelength of 1550 nm.

formed of silica. The structure parameters are as follows: the pitch $\Lambda = 2.05$ μm, the air hole diameter $d = 1.7$ μm, and the central core diameter $d_c = 1.4$ μm.

Figure 1(b) shows the fundamental mode intensity $\|\hat{e}(r_\perp)\|$ inside the optical fiber at $\lambda = 1550$ nm. Because of the specific symmetry of PCF, the birefringence does not exist in the waveguide. As seen from Fig. 1(b), because of the large refractive index contrast between the tellurite glass core and the silica cladding, the light energy is almost confined to the central core region, and the z-component of the fundamental mode turns out to be visible. Furthermore, the mode profile changes obviously within a wavelength range. This instability of the mode profile leads to the suppression of RSSFS. This strong field confinement produces a much smaller effective model field area and a larger Kerr nonlinearity coefficient than that of a silica core.

Far away from the resonances of the medium, the refractive index of tellurite glass can be approximated by the Sellmeier equation:

$$n^2(\lambda) = 1 + \frac{B_1\lambda^2}{\lambda^2 - C_1} + \frac{B_2\lambda^2}{\lambda^2 - C_2} + \frac{B_3\lambda^2}{\lambda^2 - C_3}, \tag{1}$$

where B_1, B_2, B_3, C_1, C_2, and C_3 are the material constants. For tellurite glass T2, these parameters are 0.71, 1.28, 1.28, 9.85×10^4 nm^2, -3×10^4nm^2, and -3×10^4 nm^2.[17] Using the finite element method, the calculated group velocity dispersion (GVD) curve is presented in Fig. 2, where the first zero dispersion wavelength is 0.9 μm, and the second one is beyond consideration.

Because the light is mainly confined to the tellurite core, the material dispersion of tellurite glass T2 dominates the vast majority of the dispersion. The holes in the cladding

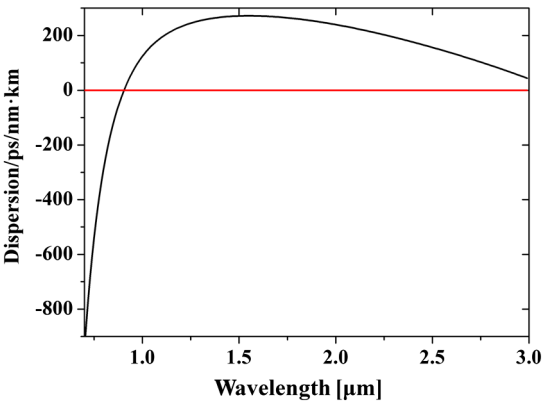

Fig. 2 Group velocity dispersion curve of the fundamental mode of the proposed PCF.

can considerably modify the GVD. This PCF structure can exhibit a wide region of anomalous dispersion and locate the maximum of the geometrical nonlinear coefficient inside the region of anomalous dispersion. This is very important for observing the visible suppression phenomenon of RSSFS.

We have analyzed many different fiber core materials and fiber structures, and compared the optical properties such as GVD, Kerr nonlinearity, and geometrical nonlinearity. Our choice of core material and PCF parameters has been dictated by two conditions which cannot easily be simultaneously met. The first requirement is that there must be a relatively large refractive index contrast between the core and cladding, so that the magnitude of the longitudinal component of the electric field becomes appreciable. The second requirement is that the holes should considerably modify the GVD in such a way that the maximum of the geometrical nonlinear coefficient is located inside the region of anomalous dispersion. At last, we find that the designed fiber is the most suitable to exhibit the suppression of RSSFS.

Defining the first moment of the nonlinear response function in tellurite glass as:

$$T_R = f_R \left.\frac{d[\mathrm{Im}h_R(\Delta\omega)]}{d(\Delta\omega)}\right|_{\Delta\omega=0}, \tag{2}$$

where $f_R = 0.51$ represents the fractional contribution of the delayed Raman response to the nonlinear polarization in tellurite glass,[18] $h_R(\Delta\omega)$ described in Ref. 17 is the Fourier transform of the Raman response function $h_R(t)$, and T_R is estimated to be 1.32 fs in the proposed PCF.

3 Theory Model for Pulse Propagation

In the derivation, the normalized field profile of fiber eigenmodes $\hat{e}_\lambda(r_\perp, \lambda)$ is spread into a Taylor series at the central wavelength λ_0

$$\hat{e}_\lambda(r_\perp, \lambda) = \sum_{j\geq 0} \frac{1}{j!} f^j_{\lambda_0}(r_\perp)\left(\frac{\Delta\lambda}{\lambda_0}\right)^j, \tag{3}$$

where $\Delta\lambda$ is the wavelength detuning between λ and λ_0. $f^j_{\lambda_0} = [\lambda_0^j \partial^j \hat{e}_\lambda(r_\perp, \lambda)/\partial\lambda^j]_{\lambda=\lambda_0}$ is the j'th term of Taylor expansion. $\hat{e}_\lambda(r_\perp, \lambda)$ is a vector field and its z-component is comparable with the other two transverse components

when the core diameter is sufficiently small or the refractive index contrast between core and cladding is large enough. Thus, the z-component must be taken into account. By spreading the fiber eigenmodes into the Taylor series, the z-component of electric fields can be well contained in the derivation of GNLSE. Then, the derivation is the same as Ref. 16.

A new pulse propagation equation in the PCF of silica core is obtained:

$$i\partial_z A + D(i\partial_t)A + \gamma_0\left[\left(1+\frac{i}{\omega_0}\partial_t\right)|A|^2A - T_R A\partial_t|A|^2\right] + \frac{4i\gamma_1}{\omega_0}|A|^2\partial_t A = 0. \quad (4)$$

Here, A is the electric field envelope, ω_0 is the angular frequency at λ_0, $D(i\partial_t)$ is the conventional fiber GVD, γ_0 is the Kerr nonlinearity coefficient, and γ_1 is the geometrical nonlinearity coefficient,

$$\gamma_1(\lambda_0) = \frac{3}{16ct_0}\int \chi^{(3)}_{xxxx}(r_\perp)[f^{*(1)}_{\lambda_0}f^{(0)}_{\lambda_0}|f^{(0)}_{\lambda_0}|^2]\mathrm{d}r_\perp. \quad (5)$$

Here, $\chi^{(3)}_{xxxx}(r_\perp)$ is the third-order susceptibility determined by the transverse coordinates of the waveguide, and t_0 is the pulse duration.

It can be found from Eq. (4) that there is a new term of geometrical nonlinearity compared to the conventional GNLSE. This new term is deduced from the non-neglectful z-component of electric fields and can give a suppression of RSSFS.

Considering Eq. (4) in PCF with the tellurite core, two improvements are made. First, because the tellurite glasses have a higher fiber loss than that of silica glass, the fiber loss α of the tellurite glass should be considered to ensure the result to be more accurate. Second, only the first three-order Taylor expansions are considered because the pulse central wavelength is far away from the zero dispersion wavelength of PCF.

By a few derivations, the final pulse propagation equation in PCF with the tellurite subwavelength core is obtained as the following

$$i\frac{\partial A}{\partial z} + \frac{i}{2}\alpha A - \frac{\beta_2}{2}\frac{\partial^2 A}{\partial T^2} - \frac{i\beta_3}{6}\frac{\partial^3 A}{\partial T^3} + \gamma_0\left[|A|^2A + \frac{i}{\omega_0}\frac{\partial}{\partial T}(|A|^2A) - T_R A\frac{\partial|A|^2}{\partial T}\right] + \frac{4i\gamma_1}{\omega_0}|A|^2\frac{\partial A}{\partial T} = 0, \quad (6)$$

where $\alpha = 2$ dB/m in the tellurite glass T2, and β_2 and β_3 are the second and third-order GVD coefficients. Other parameters are defined the same as in Eq. (4).

The curves of γ_0 and γ_1 are presented in Fig. 3. Black and red lines indicate that γ_0 and γ_1 are plotted versus wavelength. It can be seen that γ_0 decreases monotonically as the radiation wavelength increases, while γ_1 shows a different trend. γ_1 increases up to the maximum value at a wavelength of 1.8 μm and reduces monotonically after that.

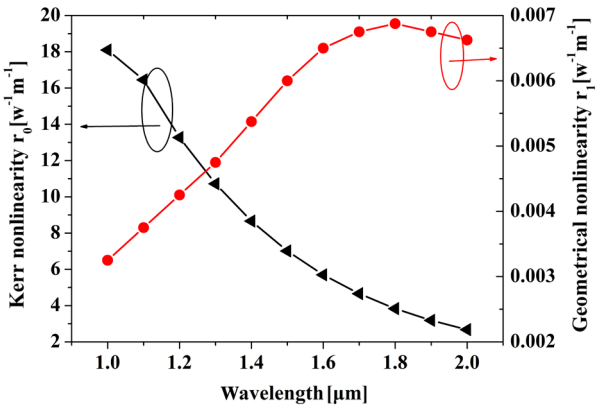

Fig. 3 Kerr nonlinearity coefficient and geometrical nonlinearity coefficient in the designed PCF.

4 Suppression of Raman Soliton Self-Frequency Shift

Now the influence of γ_1 on the RSFS of solitons is shown. It impacts on the soliton propagation and results in a suppression of the RSFS. A numerical simulation of the conventional GNLSE in the same condition compared with Eq. (6) is carried out, where the new geometrical nonlinearity term is included.

The pump central wavelength is 1550 nm in the anomalous dispersion region. With an input power P, the soliton order number is $N = [\gamma_0 P t_0^2/|\beta_2|]^{1/2}$. In the first simulation, we use two different input pulses with the powers of 200 and 400 W, corresponding to soliton order numbers $N = 1$ and 2. $L = 0.2$ m is the propagation distance. The input pulse is the hyperbolic secant and has a temporal width t_0 equal to 100 fs. Figure 4 shows the output spectrum of the input pump pulse at different pump powers: (a) $P = 200$, $N = 1$ and (b) $P = 400$, $N = 2$. The blue dashed line and the red pecked line indicate the evolutions of the short pulses in the proposed PCF.

In Fig. 4, compared to the results obtained by the GNLSE, it can be clearly seen that the new geometrical nonlinearity acts on the optical solitons and leads to a suppression of the RSSFS. In Fig. 4(a), the central wavelength of the first-order soliton by the GNLSE is 1680.9 nm, and the corresponding central wavelength for the new equation is 1678.3 nm. There is a suppression of 2.6 nm when taking the geometrical nonlinearity term into consideration. In Fig. 4(b), the central wavelengths of the first- and second-order solitons by the GNLSE are 1655 and 1725.2 nm, corresponding to 1651 and 1721.3 nm with the new equation. There are a 4-nm suppression for the first-order soliton and a 3.9-nm suppression for the second-order soliton. Also, the suppression degree for $P = 400$, $N = 2$ is bigger than that for $P = 200$, $N = 1$. Because the geometrical nonlinearity only induces a suppression on the soliton evolution, the soliton shape is the same as the output by the GNLSE.

In the second simulation, two different hyperbolic secant pulses with the temporal widths of 100 and 150 fs are used. The input powers are 100 W, and the propagation distance is 0.25 m.

Figure 5 shows the output spectra of the input pump pulse at different temporal widths: (a) $t_0 = 100$ fs, $N = 1$, (b) $t_0 = 150$ fs, $N = 1$. It is easy to see that the solitons propagate the same distance at the different pulse durations. When

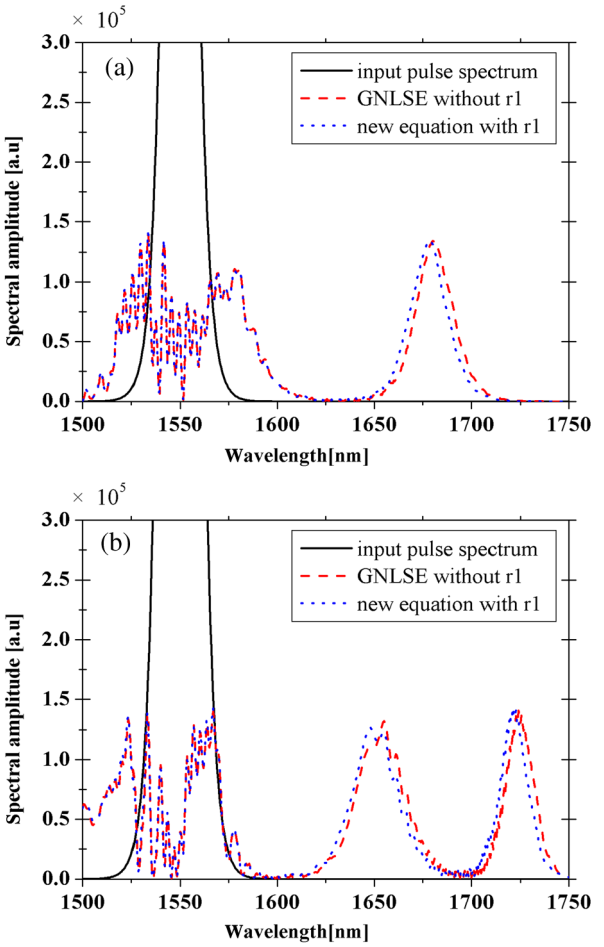

Fig. 4 Simulation of light propagation in the proposed PCF: (a) $P = 200$, $N = 1$, and (b) $P = 400$, $N = 2$.

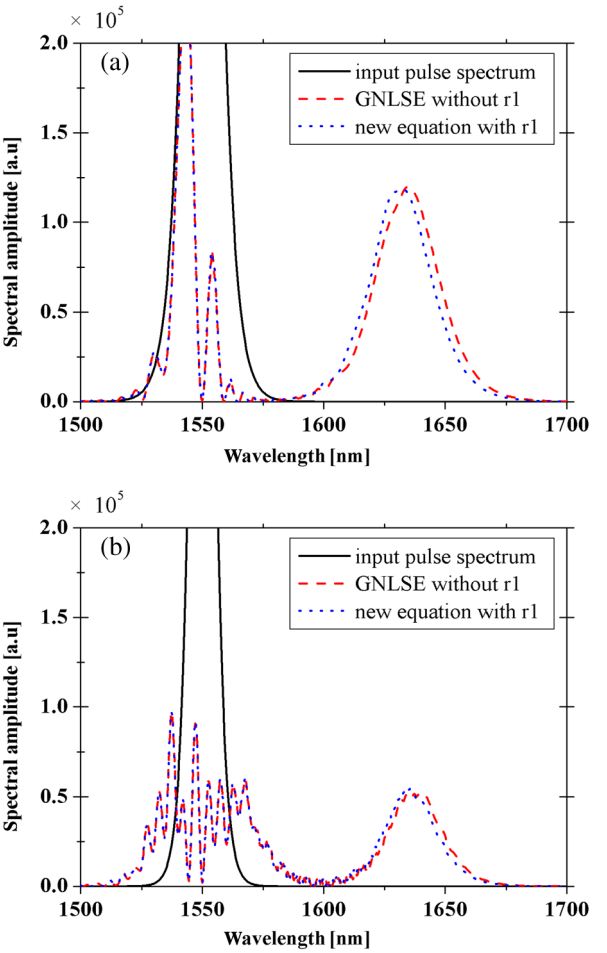

Fig. 5 Simulation of light propagation in the proposed PCF: (a) $t_0 = 100$ fs, (b) $t_0 = 150$ fs.

the pump temporal width $t_0 = 100$ fs, the central wavelengths of solitons are 1634.9 and 1630 nm for the GNLSE and the new equation, a 4.9-nm suppression emerging. When the pump temporal width $t_0 = 150$ fs, the central wavelengths are 1638.5 and 1636.1 nm, and there is a 2.4-nm suppression. When the temporal width is shorter, the suppression phenomenon of RSSFS is more remarkable.

In the third simulation, we simulate the output spectra at different transmission distances of 0.2, 0.4, and 1 m, respectively. The input powers are 100 W, and the pump temporal width is 100 fs. Figure 6 shows the output spectra for $N = 1$ at (a) $L = 0.2$ m, (b) $L = 0.4$ m, and (c) $L = 1$ m. Corresponding to (a) $L = 0.2$ m, (b) $L = 0.4$ m, and (c) $L = 1$ m, the central wavelengths for the GNLSE are 1632.8, 1638.7, and 1639.9 nm, and the central wavelengths for the new equation are 1628.6, 1635.5, and 1637.1 nm. The suppressions of 4.2, 3.2, and 2.8 nm are obtained. When the transmission distance increases from 0.2 to 1 m, the suppression is reduced to 2.8 nm. Due to the combined action of the GVD and SPM, when the pulses are propagated in the waveguide, the soliton can be compressed. The suppression degree of RSSFS is more visible as L increases.

5 Discussion on Fabrication

In the actual case, it is more difficult to fabricate tellurite glass fibers than silica fibers due to the smaller working temperature range. When the glass crystallization temperature T_x is close to the glass transition temperature T_g, the thermal expansion coefficient is increased, and the thermostability is decreased. The small working temperature range causes a degradation of the optical performance in the drawing process of the fiber. By proportionally doping the rare earth element, T_x and T_g can be optimized, and the working temperature range can be enlarged. The tellurite glass T2 has a T_x of 45°C and a T_g of 278°C. The working temperature range is as wide as 179°C. Also, this big working temperature range can decrease the thermal expansion coefficient and increase the thermostability of the glass. Moreover, the glass optical performance including the nonlinear refractive index, dispersion, and losses are stable in the drawing process of the fiber.

For the fabrication of the tellurite-glass subwavelength core PCF, we have used the improved stacking method and the center vacuumizing method. In the case of the optimized drawing speed and temperature, the size of the core can be controlled by adjusting the extract pressure. Although the melting temperature of T2 [$77TeO_2$-$10Na_2O$-10ZnO-3PbO (%mol)] is lower than that of silica, the subwavelength core PCF can be obtained using a rapid drawing method (7 to 10 mm/ min). In order to decrease the core size and avoid the collapsing of the air holes, the draw speed and temperature must be optimized and the extract pressure should be decreased.

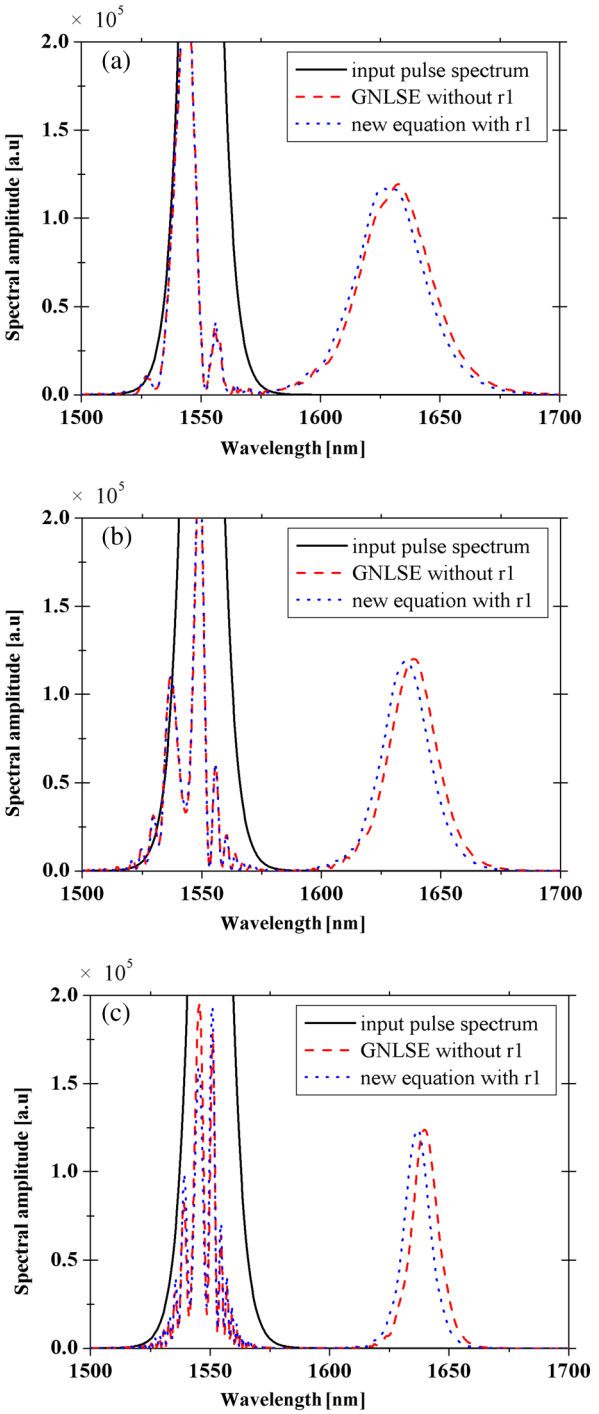

Fig. 6 Simulation of light propagation in the proposed PCF (a) $L = 0.2$ m, (b) $L = 0.4$ m, and (c) $L = 1$ m.

6 Conclusion

In summary, the suppression of RSSFS in PCF with the tellurite subwavelength core induced by the new geometrical nonlinearity is demonstrated. The effects of the pulse width, the pump power, and the propagation distance on the suppression of RSSFS are analyzed. The simulation conditions chosen are close to the physical truth, and the obtained results are much more precise. Moreover, the suppression effect on the fundamental soliton is more remarkable than the high-order soliton. Our results more powerfully prove the existence of the new geometrical nonlinearity. It is shown that the geometrical nonlinearity is strongly dependent on the geometrical structure of PCF. It can also be expected that the geometrical nonlinearity may have a particular influence on the spectral components generated at the short wavelength.

Acknowledgments

This work is partly supported by the National Basic Research Program (2010CB327605), the National Natural Science Foundation of China (61307109), the National High-Technology Research and Development Program of China (2013AA031501), the key grant of Ministry of Education (109015), the Program for New Century Excellent Talents in University (NECT-11-0596) and Beijing Nova program (2011066), the Specialized Research Fund for the Doctoral Program of Higher Education (20120005120021), the Fundamental Research Funds for the Central Universities (2013RC1202), the China Postdoctoral Science Foundation (2012M511826), the Postdoctoral Science Foundation of Guangdong Province (244331).

References

1. J. Broeng and D. Mogilevtsev, "Photonic crystal fibers: a new class of optical waveguides," *Opt. Fiber Technol.* **5**(3), 305–330 (1999).
2. J. Limpert et al., "High-power air-clad large-mode-area photonic crystal fiber laser," *Opt. Express* **11**(7), 818–823 (2003).
3. L.-P. Shen, W.-P. Huang, and S.-S. Jian, "Design of photonic crystal fibers for dispersion-related applications," *J. Lightwave Technol.* **21** (7), 1644–1651 (2003).
4. R. K. Sinha and S. K. Varshney, "Dispersion properties of photonic crystal fibers," *Microwave Opt. Technol. Lett.* **37**, 129–132 (2003).
5. J. C. Knight et al., "Anomalous dispersion in photonic crystal fiber," *IEEE Photonics Technol. Lett.* **12**(7), 807–809 (2000).
6. J. Y. Y. Leong et al., "High-nonlinearity dispersion-shifted lead-silicate holey fibers for efficient 1 μm pumped supercontinuum generation," *J. Lightwave Technol.* **24**(1), 183–190 (2006).
7. X. Sang, P. L. Chu, and C. Yu, "Applications of nonlinear effects in highly nonlinear photonic crystal fiber to optical communications," *Opt. Quantum Electron.* **37**(10), 965–994 (2005).
8. T. Südmeyer et al., "Nonlinear femtosecond pulse compression at high average power levels by use of a large-mode-area holey fiber," *Opt. Lett.* **28**(20), 1951–1953 (2003).
9. J. van Howe et al., "Demonstration of soliton self-frequency shift below 1300 nm in higher-order mode, solid silica-based fiber," *Opt. Lett.* **32**(4), 340–342 (2007).
10. A. Ortigosa-Blanch, J. C. Knight, and P. S. J. Russell, "Pulse breaking and supercontinuum generation with 200-fs pump pulses in photonic crystal fibers," *J. Opt. Soc. Am. B* **19**(11), 2567–2572 (2002).
11. T. Yamamoto, H. Kubota, and S. Kawanishi, "Supercontinuum generation at 1.55 μm in a dispersion-flattened polarization-maintaining photonic crystal fiber," *Opt. Express* **11**(13), 537–1540 (2003).
12. Z. Zhu and T. G. Brown, "Experimental studies of polarization properties of supercontinua generated in a birefringent photonic crystal fiber," *Opt. Express* **12**(5), 791–796 (2004).
13. X. Feng et al., "Single-mode tellurite glass holey fiber with extremely large mode area for infrared nonlinear applications," *Opt. Express* **16** (18), 13651–13656 (2008).
14. R. F. Souza et al., "Femtosecond nonlinear optical properties of tellurite glasses," *Appl. Phys. Lett.* **89**(17), 171917 (2006).
15. M. Liao et al., "Tellurite microstructure fibers with small hexagonal core for supercontinuum generation," *Opt. Express* **17**(14), 12174–12182 (2009).
16. T. Truong, X. Tran, and F. Biancalana, "An accurate envelope equation for light propagation in photonic nanowires: new nonlinear effects," *Opt. Express* **17**, 17934–17949 (2009).
17. M. D. O'Donnell et al., "Tellurite and fluorotellurite glasses for fiber optic raman amplifiers:glass characterization, optical properties, raman gain, preliminary fiberization, and fiber characterization," *J. Am. Ceram. Soc.* **90**(5), 1448–1457 (2007).
18. X. Yan et al., "Transient Raman response and soliton self-frequency shift in tellurite microstructured fiber," *J. Appl. Phys.* **108**, 123110 (2010).

Shuai Wei received his bachelor's and master's degrees in Shandong University of Science and Technology, Qingdao, China. Also, he is currently pursuing his PhD in the State Key Laboratory of Information Photonics and Optical Communications, Beijing University of Posts and Telecommunications, China. His research focuses on nonlinear fiber optics and photonic crystal fibers.

Jinhui Yuan received his MS in science and technology of electrons in optics engineering from Yanshan University, Qinhuangdao, China, in 2008. Also, he received his PhD in physics electronics from the Beijing University of Posts and Telecommunications, Beijing, China, in 2011. His current research interests include investigation on photonic crystal fibers, silicon waveguide, and optical-fiber devices.

Chongxiu Yu is a professor of State Key Laboratory of Information Photonics and Optical Communications. Her research interests are the optical-fiber communication and lightwave technology, photonic switching, optoelectronics technology, and its applications. She is a member of Chinese Institute of Communication, Committee of Fiber Optics and Integral Optics, Chinese Optical Society, and SPIE.

Sha Li received her bachelor's and master's degrees in Hainan University of Technology, and is currently pursuing a PhD in Beijing University of Posts and Telecommunications, China. Her research focuses on high-speed all-optical sampling and high-speed optical communication.

Boyuan Jin received his bachelor's degree in telecommunication engineering, South China University of Technology, and is currently pursuing his PhD in the State Key Laboratory of Information Photonics and Optical Communications, Beijing University of Posts and Telecommunications, China. His research focuses on nonlinear fiber optics and high-speed optical communication.

Xiaoming Hu received his bachelor's and master's degrees in Hainan University of Technology in Beijing University of Posts and Telecommunications, and is currently pursuing his PhD in Beijing University of Posts and Telecommunications, China. His research focuses on photonic crystal fibers and high-speed optical communication.

Gerald Farrell is the director of the Photonics Research Centre at the DIT (Dublin institute of technology), PhD, and MIEI. His research is focused on the area of photonics, in particular optical sensing, FBG interrogation systems, modeling, and applications of fiber bend loss, SMS, and PLC-based edge filters.

Qiang Wu received his PhD in Beijing University of Posts and Telecommunications. Now, he works at Dublin Institute of Technology as a teacher. His research is focused on the area of photonics. His specific areas of interest are fiber sensors and fiber gratings, surface plasmon resonant, and optical waveguide laser.